Applied Surface Science 357 (2015) 55–59

Contents lists available at ScienceDirect

Applied Surface Science

journal homepage: www.elsevier.com/locate/apsusc

Reconstructed graphene nanoribbon as a sensor for nitrogen based molecules

Neeraj K. Jaiswal[a], Goran Kovačević[b,*], Branko Pivac[b]

[a] Discipline of Physics, Indian Institute of Information Technology Design & Manufacturing, Jabalpur 482005, India
[b] Ruđer Bošković Institute, Bijenička 54, P.O. Box 180, HR-10002 Zagreb, Croatia

ARTICLE INFO

Article history:
Received 21 July 2015
Accepted 25 August 2015

PACS:
68.43.Bc
68.43.Fg
68.65.Pq
72.80.Vp

Keywords:
Graphene nanoribbon
Reaction mechanism
Conductivity
Density of states
DFT
MP2

ABSTRACT

The usage of reconstructed zigzag graphene nanoribbon (RZGNR) as a sensor for nitrogen based chemicals is being analyzed. The principle of sensing is based on reaction of nitrogen atom with the edge of RZGNR, which causes a measurable change in electrical properties of the nanoribbon. In order to characterize the RZGNR based sensor, reaction mechanisms of a graphene nanoribbon with an ammonia molecule (NH_3) are analyzed in detail by using *ab initio* and DFT calculations. Ammonia molecule reacts with RZGNR via a two stage reaction. The first stage represents the rate limiting step of the entire reaction and produces a reaction intermediate. The reaction intermediate undergoes proton transfer as a second stage reaction in order to form energetically stable product. The negative differential resistance (NDR) behavior was noticed in our model of RZGNR. Upon reaction with the NH_3 molecule, the electronic properties of RZGNR are significantly modified and the observed NDR behavior disappears. Present findings show that adsorption of guest NH_3 molecule can be sensed by the change in current passing through the ribbons.

1. Introduction

Being a perfect 2-D material, graphene is considered to be a promising agent for the sensing applications [1–6]. A monolayer of graphene is capable of detecting individual molecules, adsorbed from gas phase [1] or even larger molecules that would be attached to a graphene sheet from solution, indicating its applicability in sensing wide range of molecules [3–7], or even biomolecules [8,2,9–11]. Chemically modified graphene sheets like graphene oxide, doped graphene, functionalized graphene nanoribbons (GNR) also pledge for applications in advanced sensors since chemical modifications provide active sites for molecular adsorption, increasing its binding energy [12]. Graphene nanoribbons (GNR) enjoy the presence of edges along with the high surface to volume ratio. These edges provide chemically active sites for the adsorption of gas molecules and therefore could play a crucial role in sensing applications. Zigzag graphene nanoribbons (ZGNR) have been preferred over armchair graphene nanoribbons (AGNR) due to their intrinsic magnetic ground state [13]. Till now, GNR with different edge terminations have been investigated and it is observed that their electronic properties are highly dependent upon the terminating element/functional groups [14,15]. This inspired researchers to investigate different edge terminations of GNR and consequently reveal their potential applications. H-terminated GNR have been extensively explored due to enhanced stability and are still dominating. Further, it is reported that termination of ribbon edges with more than one H atom, can also be used to tailor their magnetic/electronic properties. On the other hand, in-depth understanding of bare GNR is still limited. Though, few attempts have been made to explore the structural and electronic properties of bare GNR [16,17], however, detailed investigations are yet to be made. Recently, Koskinen at al. revealed that a bare ZGNR undergo strong reconstruction due to highly reactive nature of their edges [18]. It was reported that the observed reconstruction of bare edges plays a crucial role for the structural stability of the ribbon. Recently, graphene sheet without H-terminated edges has been experimentally produced via vacuum sputtering by He et al. [19]. They found about 80% reduction in the edge C—C bond lengths which is in consistence with the previous theoretical predictions. The relative stability of these spontaneously reconstructed graphene edges suggests that these types of structures should be

* Corresponding author.
E-mail addresses: neerajkjaiswal@gmail.com (N.K. Jaiswal), gkova@irb.hr (G. Kovačević), pivac@irb.hr (B. Pivac).

http://dx.doi.org/10.1016/j.apsusc.2015.08.219
0169-4332/

explored further for more realistic predictions of graphene based devices.

Motivated from this, we have investigated the reaction mechanism and the energetics for reaction between ammonia (NH_3) and the edge of reconstructed ZGNR (RZGNR) as well as the electronic and transport properties of reaction product for the application of NH_3 sensors. The choice of NH_3 lies in the fact that it is the simplest compound that can be considered as a model for hazardous nitrogen-based compounds. NH_3 itself is a toxic gas that can be severely dangerous for the human being. Thus, it is necessary to detect its early stage leakage (if any) to avoid any mishap incident.

2. Theoretical methods

For the calculation of electronic and transport properties, we performed calculations based on density functional theory (DFT) as implemented in ATK-VNL [20,21]. First, the geometry optimization was performed with a force tolerance of 0.02 eV/Å. The ribbons were modeled with periodic boundary conditions. A vacuum region of 10 Å was introduced between different RZGNR in neighboring periodic replicas. The number of k-points taken along the infinite dimension of RZNGR were 50 and a mesh cut off energy of 50 Ryd was selected for the present calculations. The Generalized Gradient Approximation (GGA.PBE) as proposed by Perdew, Burke and Ernzerhof (PBE) [22] was used to account the exchange correlation effects. The transport calculations of the considered geometries were carried out using non-equilibrium Green's function (NEGF) coupled with DFT [20,21].

Reaction mechanisms were determined by employing Gaussian orbital based DFT on the search for stationary points on the potential energy surface (minima and transition states). The search for stationary points was done on the non-periodic cluster models. M06-2X hybrid meta exchange functional [23] and second order Møller–Plesset perturbation theory (MP2) [24] with 6-31G(d,p) basis set were used. M06-2X functional was proven to be one of the best DFT functionals for thermochemistry, kinetics and non-covalent interactions [23] and, therefore is very well suited for the determination of reaction mechanisms. On the other hand, MP2 calculations provide a way for treating electronic correlation effects through the perturbation theory and is used to verify reaction mechanism, obtained with M06-2X. Frequencies are calculated on all optimized stationary points in order to prove their nature (existence of a single imaginary frequency for transition states and none for minima). For all transition states, atomic motions along normal modes that correspond to imaginary frequencies were visualized in order to check that converged geometries are desired transition states. In cases where additional imaginary frequencies of low magnitude were obtained, atomic motions along corresponding normal modes were also analyzed in order to check if they correspond to large amplitude motions. Intrinsic reaction coordinate (IRC) calculations were done on all transition states in order to unambiguously proof that obtained transition states were connecting right minima. Single point calculations were computed on M06-2X converged stationary points by using second order MP2 theory. The basis set, that was used in geometry optimizations (6-31G(d,p)) was also used in single point calculations (MP2/6-31G(d,p)). All calculations on cluster models were done with the GAMESS [25,26] program package.

3. Results and discussion

3.1. Reaction mechanism

Unlike infinite graphene sheets, graphene nanoribbons are characterized by their edge. We used the zz(57) reconstructed graphene edge, published by Koskinen et al. [18] since it is energetically the most stable. The zz(57) is characterized by repeating heptagons and pentagons along the edge. Each heptagon have two two-valent carbon atoms in bend coordination, that are exposed in the edge of a graphene nanoribbon. The bond between these two atoms is unusually short (1.24 Å) [18], indicating a triple bond character. Two-valent carbon atoms with similar bonding, in unstrained conditions (like acetylene) have a linear (unbend) coordination. The strained atomic pair on the zz(57) edge is the most reactive place on a nanoribbon since a potential reaction on this place would change the linear coordination of two-valent carbon atoms into a trigonal planar and consequently, reduce a strain. Reaction on any other atom in graphene would change its coordination from the trigonal planar into a tetrahedral one, which would introduce a strain.

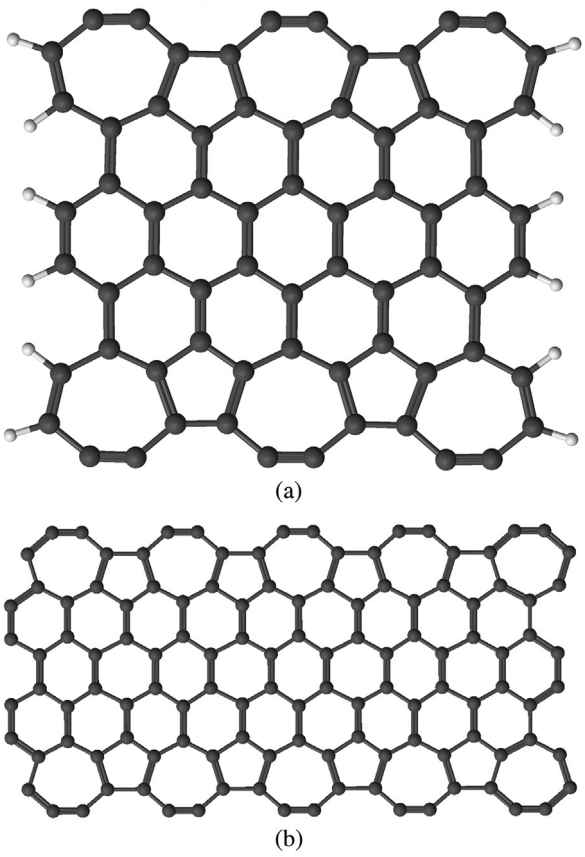

Fig. 1. Atomic models used in calculations of graphene nanoribbons: (a) cluster model of graphene nanoribbon, terminated with hydrogen atoms and (b) periodic model, used in calculations with periodic boundary conditions.

We modeled reaction of ammonia molecule with the atomic pair with the triple bond, the most reactive site of a graphene nanoribbon. The cluster model of a RZNGR was chosen as a 12 Å long piece, terminated with hydrogen atoms (Fig. 1a). Its edge contains three triple bonds. The middle triple bond in the cluster model is used for reaction modeling since in this way, the triple bonds on both sides from the reaction center provide large padding.

The reaction of an ammonia molecule with zz(57) edge of the graphene nanoribbon proceeds in two reaction steps. The first step is an addition of the ammonia molecule into a triple bond. Minimum energy path for the addition reaction passes through a prereaction complex (**1**) (see Fig. 2a). This complex represents a shallow minimum about 1 meV below reactants (without zero-point vibrational energy). In this complex, there are no chemical bonds between ammonia molecule and RZNGR. The energy stabilization of **1** comes from dispersion forces only.

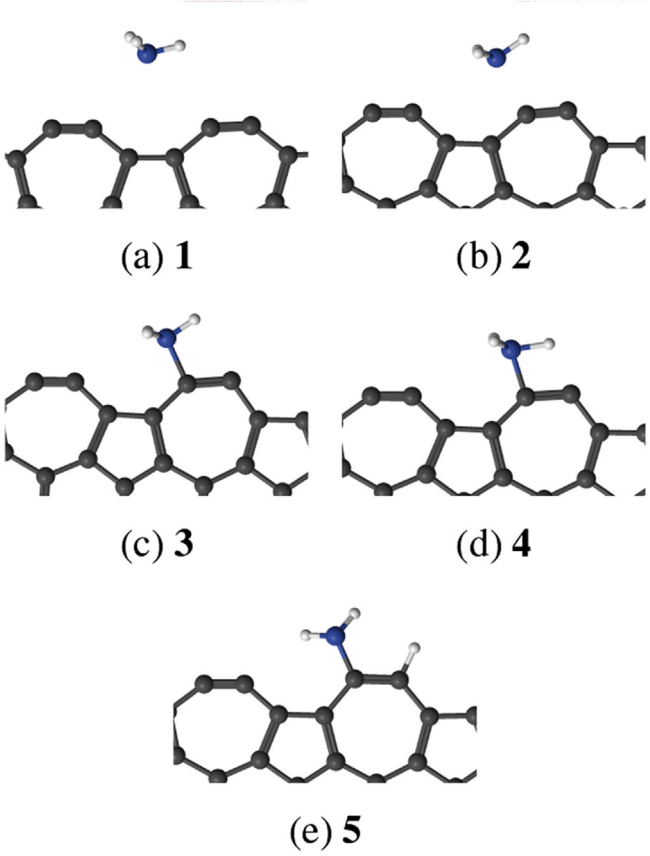

Fig. 2. Geometries of stationary points on the reaction path for addition of ammonia molecule onto a zz(57) edge of a reconstructed graphene nanoribbon. Only the reaction center is shown for clarity. (a) Prereaction complex; (b) transition state; (c) intermediate minimum; (d) transition state; and (e) global minimum.

The first transition state **2** (Fig. 2b) represents the largest energy barrier on the reaction path (see Fig. 3) and, therefore is the rate determining step of the entire reaction. In the transition state the seven-membered ring in the reaction center is being distorted. That distortion is governed by the change in the bonding pattern of carbon atoms in the reaction center. The carbon atom in the reaction center has one emerging bond with the nitrogen atom in the ammonia molecule which causes a reduction in bond order of the triple bond. After the C—N bond is formed, the bond that was initially

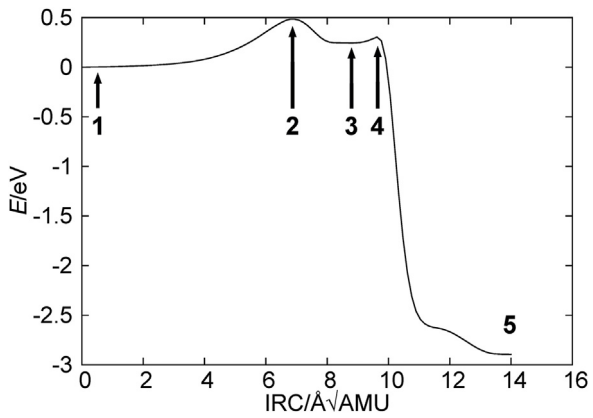

Fig. 3. Energy profile along intrinsic reaction coordinate (IRC) for the reaction between NH_3 and reconstructed zigzag graphene nanoribbon. Energies are calculated with MP2/6-31G(d,p) level of theory. Geometries that correspond to the stationary points (**1**–**5**) are shown in Fig. 2.

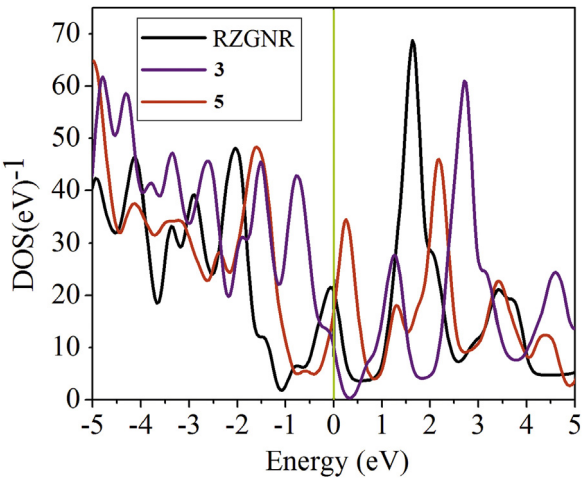

Fig. 4. The calculated DOS profiles for RZGNR and that of structures, reconstructed zigzag graphene nanoribbon upon reaction with ammonia (**5**) and reaction intermediate (**3**).

triple, elongates in the reaction intermediate **3** (see Fig. 2c) from 1.24 Å to 1.35 Å, as a result of a reduced bond order.

The second reaction step represents the proton transfer from the nitrogen atom to the carbon atom in the reaction center, that did not react yet. The corresponding transition state **4** (Fig. 2d) is in the form of four-membered ring, created by the moving hydrogen atom. That transition state is lower than the first one (**2**), allowing the transformation of intermediates **3** with enough energy towards the product **5** (Fig. 2e). Since the intermediate **3** was created from the ammonia molecule with enough energy to surpass the energy barrier represented by the transition state **2**, the intermediate should have that energy available in the form of vibrational degrees of freedom for passing through the transition state **4**, which makes **3** a short-lived species. The product **5** is energetically stabilized for almost 3 eV with respect to the reactants. Such a high energy stabilization represents an impassable barrier for reverse reaction at room temperature. Therefore the product **5** is a stable species that can last for a long time, enough for determination of its electrical properties.

3.2. Electronic and transport properties

The RZGNR can be used for the sensing applications if the changes in the electronic properties due to NH_3 adsorption could be detected. In order to compare electronic properties of RZNGR, **3** and **5**, periodic models of their structures were optimized (see Fig. 1b) and electronic properties were calculated on these geometries. **3** was taken into account since some nitrogen-based molecules with a fully substituted nitrogen atom might lack the second stage reaction. Therefore, to observe the electronic properties of RZGNR along with that of **3** and **5**, we have calculated the electronic density of states (DOS) as depicted in Fig. 4. We observed a finite DOS across the Fermi level for all the structures indicating towards their metallic character. Moreover, in the vicinity of Fermi level, highest availability of electronic states is noticed for **5** whereas the difference in DOS for remaining structures is not much significant. The highest valence band peak in the energy range 0 to −1.5 eV is contributed of **5** followed by two small peaks of **3**. Further, a number of peaks are observed in the valence as well as conduction band. The central peak in the vicinity of Fermi level is significantly enhanced in **5** which is slightly shifted towards conduction band region and indicates larger availability of DOS for electronic conduction. Thus, the observed NH_3 assisted changes in the electronic DOS of RZGNR are significant to be utilized for sensing applications.

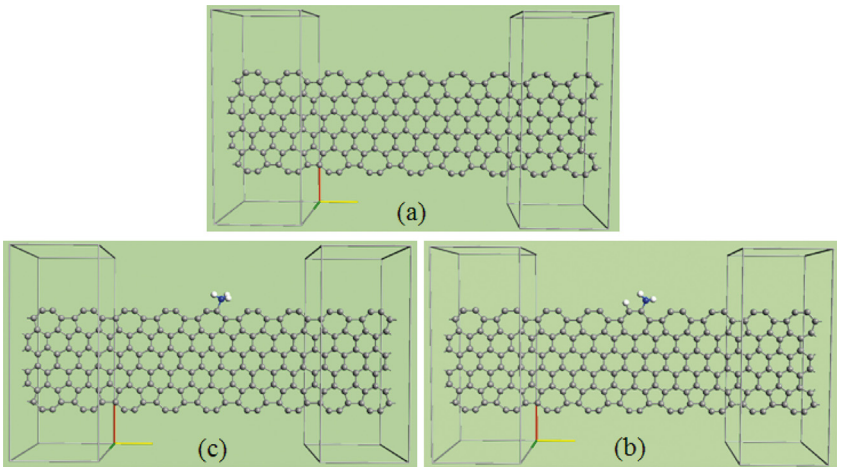

Fig. 5. The schematics of two-probe geometries used to calculate *I–V* characteristics for (a) reconstructed zigzag graphene nanoribbon, (b) structure **3**, and (c) structure **5**.

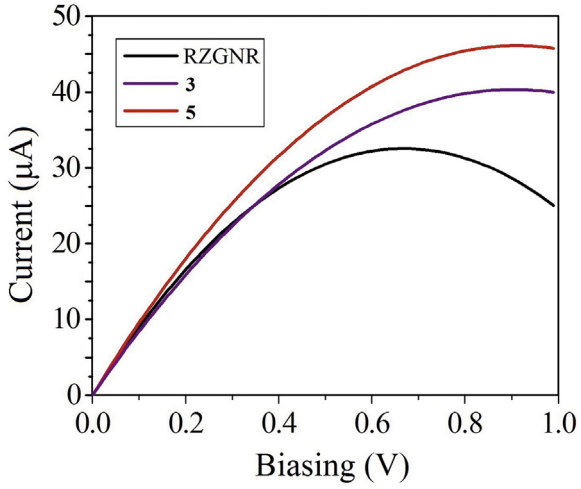

Fig. 6. The calculated *I–V* characteristics for RZGNR along with that of **3** and **5**.

In order to investigate the effect of this change on some measurable physical quantity, we also calculated the current–voltage (*I–V*) characteristic of these structures. The two-probe geometries, employed to calculated the (*I–V*) behavior are presented in Fig. 5.

There are three parts of two-probe geometry, the central scattering region along with left and right electrodes. These electrodes are seamlessly coupled with central region to minimized the interface mismatching. The calculated *I–V* characteristics of RZGNR, **3** and **5** are displayed in Fig. 6. The *I–V* relationship of RZGNR shows a sharp rise with increasing the voltage up to 0.6 V. Once the current has attained a maximum value of about 32 μA at 0.65 V, it starts decreasing with further increment in the bias voltage. Thus, a negative differential resistance (NDR) is observed for RZGNR (Fig. 6). To the best of our knowledge, this is probably the first report on NDR behavior noticed in proposed RZGNR device. However, the same has also been observed in ideal GNR, silicene and boron nitride nanoribbons [27,15,28]. As the crumpling is intrinsic phenomenon in perfect 2-D sheet of graphene [29,30], the observed NDR behavior in RZGNR would be more promising than that in perfect GNR. Moreover, it is revealed that the current value is significantly enhanced beyond 0.6 V in **3** as well in **5**. Up to 0.8 V of applied bias, there is a sharp rise in the current value for both the structures (**3** and **5**) beyond which, the current increases at a slow pace. Moreover, the magnitude of current is found higher for **5** than that of **3**. At 1 V of applied bias, the current approaches to 40 μA and 45 μA for **3** and **5**, respectively. Thus, NH_3 assisted changes are remarkable on the *I–V* characteristics of RZGNR. As expected, the highest current is noticed for **5** which also exhibit the largest availability of electrons.

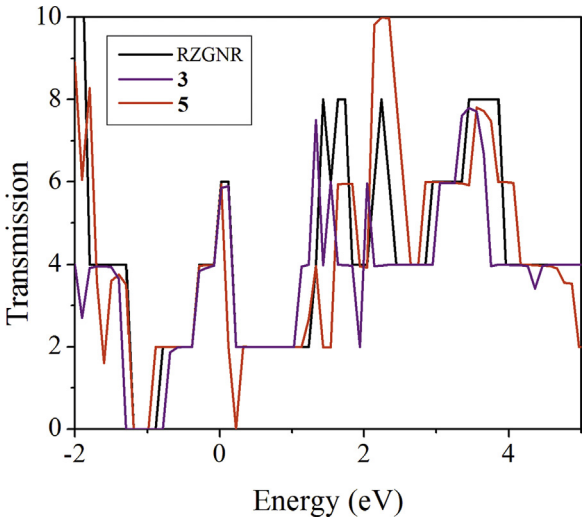

Fig. 7. The calculated transmission spectra for RZGNR along with that of **3** and **5** at 0 bias.

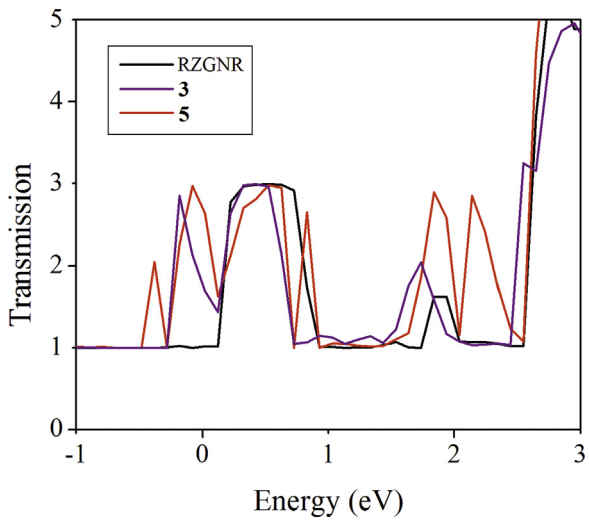

Fig. 8. The calculated transmission spectra for RZGNR along with that of **3** and **5** at 1 V bias.

For a further verification of the observed *I–V* behavior, we calculated transmission spectra (TS) for 0 bias (Fig. 7) (when no biasing is applied between the left and right electrodes) and for 1 V biasing (Fig. 8). Interestingly, when no biasing is applied, all the structures exhibit equal transmission coefficient (TC) at the Fermi level. However, the application of bias voltage between the electrodes results in non-uniform TC across the Fermi level (Fig. 8). Moreover, the highest TC at the Fermi level is observed for **5** followed by **3** and RZGNR. Thus, highest current value for **5** is defended by the corresponding high TC.

4. Conclusions

Conclusively, it is revealed that the reaction path for interaction of RZNGR with NH_3 has two transition states which makes it two-stage reaction. The first transition state is the maximum in energy along the minimal energy path making the first stage reaction the rate determining one. The lower barrier of the second stage reaction makes the reaction intermediate a short-lived species. The energy stabilization of the reaction product is significantly larger than the average thermal energy at the room temperature, which makes the reaction product a chemically stable species. RZNGR has an electronic structure with metallic character which manifests a negative differential resistance behavior. Reaction with ammonia causes significant changes in the electronic properties of RZNGR. The metallicity of RZGNR is enhanced upon NH_3 adsorption whereas the observed NDR behavior is eliminated. Significant changes in the current value pledges for the application of RZGNR towards NH_3 sensing applications.

Authors' contribution

N.K. Jaiswal conducted calculations for electronic and transport properties, wrote the manuscript; G. Kovačević did geometry optimizations and IRC calculation and prepared the manuscript; B. Pivac, Project leader, prepared the manuscript.

Acknowledgements

This work has been supported by the Croatian Science Foundation under the project 6135. Computational resources provided by Isabella cluster (isabella.srce.hr) at Zagreb University Computing Centre (SRCE) were used for this research publication. NKJ is also thankful to Indian Institute of Information Technology and Management, Gwalior, India for providing computational resources.

References

[1] F. Schedin, A.K. Geim, S.V. Morozov, E.W. Hill, P. Blake, M.I. Katsnelson, K.S. Novoselov, Detection of individual gas molecules adsorbed on graphene, Nat. Mat. 6 (2007) 652–655.
[2] R. Chowdhury, S. Adhikari, P. Rees, S.P. Wilks, Graphene-based biosensor using transport properties, Phys. Rev. B 83 (2011) 045401-1–045401-7.
[3] H.-P. Zhang, X.-G. Luo, X.-Y. Lin, X. Lu, Y. Leng, H.-T. Song, Density functional theory calculations on the adsorption of formaldehyde and other harmful gases on pure, Ti-doped, or N-doped graphene sheets, Appl. Surf. Sci. 283 (0) (2013) 559–565.
[4] E. Ashori, F. Nazari, F. Illas, Adsorption of {H_2S} on carbonaceous materials of different dimensionality, Int. J. Hydrogen Energy 39 (12) (2014) 6610–6619.
[5] Z. Chen, P. Darancet, L. Wang, A.C. Crowther, Y. Gao, C.R. Dean, T. Taniguchi, K. Watanabe, J. Hone, C.A. Marianetti, L.E. Brus, Physical adsorption and charge transfer of molecular Br_2 on graphene, ACS Nano 8 (3) (2014) 2943–2950.
[6] B.N. Papas, I.D. Petsalakis, G. Theodorakopoulos, J.L. Whitten, CI and DFT studies of the adsorption of the nerve agent sarin on surfaces, J. Phys. Chem. C 118 (40) (2014) 23042–23048.
[7] M. Zhang, C. Liao, C.H Mak, P. You, C.L. Mak, F. Yan, Highly sensitive glucose sensors based on enzyme-modified whole-graphene solution-gated transistors, Sci. Rep. 5 (2015) 1–6.
[8] Y. Shao, J. Wang, H. Wu, J. Liu, I.A. Aksay, Y. Lin, Graphene based electrochemical sensors and biosensors: a review, Electroanalysis 22 (10) (2010) 1027–1036.
[9] T. Kuila, S. Bose, P. Khanra, A.K. Mishra, N.H. Kim, J.H. Lee, Recent advances in graphene-based biosensors, Biosens. Bioelectron. 26 (12) (2011) 4637–4648.
[10] B. Akdim, R. Pachter, S.S. Kim, R.R. Naik, T.R. Walsh, S. Trohalaki, G. Hong, Z. Kuang, B.L. Farmer, Electronic properties of a graphene device with peptide adsorption: insight from simulation, ACS Appl. Mater. Interfaces 15 (5) (2013) 7470–7477, http://dx.doi.org/10.1021/am401731c.
[11] J. Song, P.S. Lau, M. Liu, S. Shuang, C. Dong, Y. Li, A general strategy to create RNA aptamer sensors using regulated graphene oxide adsorption, ACS Appl. Mater. Interfaces 6 (24) (2014) 21806–21812, http://dx.doi.org/10.1021/am502138n.
[12] H. Choi, M. Lee, S. Kim, K.-R. Lee, Y.-C. Chung, Detecting gas molecules via atomic magnetization, Dalton Trans. 43 (2014) 13070–13075.
[13] L. Pisani, J.A. Chan, B. Montanari, N.M. Harrison, Electronic structure and magnetic properties of graphitic ribbons, Phys. Rev. B 75 (2007) 064418.
[14] N. Jaiswal, P. Srivastava, Fe-doped armchair graphene nanoribbons for spintronic/interconnect applications, IEEE Trans. Nanotechnol. 12 (2013) 685–691.
[15] F.-B. Zheng, C.-W. Zhang, S.-S. Yan, F. Li, Novel electronic and magnetic properties in N or B doped silicene nanoribbons, J. Mater. Chem. C 1 (2013) 2735–2743.
[16] N. Jaiswal, P. Srivastava, First principles calculations of armchair graphene nanoribbons interacting with Cu atoms, Physica E 44 (2011) 75–79.
[17] T. Kawai, Y. Miyamoto, O. Sugino, Y. Koga, Graphitic ribbons without hydrogen-termination: electronic structures and stabilities, Phys. Rev. B 62 (2000) R16349–R16352.
[18] P. Koskinen, S. Malola, H. Häkkinen, Self-passivating edge reconstructions of graphene, Phys. Rev. Lett. 101 (2008) 115502-1–115502-4.
[19] K. He, G.-D. Lee, A.W. Robertson, E. Yoon, J.H. Warner, Hydrogen-free graphene edges, Nat. Commun. 5 (2014) 3040.
[20] J. Taylor, H. Guo, J. Wang, *Ab initio* modeling of quantum transport properties of molecular electronic devices, Phys. Rev. B 63 (2001) 0245407-1–0245407-7.
[21] M. Brandbyge, J.L. Mozos, P. Ordejon, J. Taylor, K. Stokbro, Density-functional method for non-equilibrium electron transport, Phys. Rev. B 65 (2002) 165401-1–165401-17.
[22] J.P. Perdew, K. Burke, M. Ernzerhof, Generalized gradient approximation made simple, Phys. Rev. Lett. 77 (1996) 3865–3868.
[23] Y. Zhao, D. Truhlar, The M06 suite of density functionals for main group thermochemistry, thermochemical kinetics, non-covalent interactions, excited states, and transition elements: two new functionals and systematic testing of four M06-class functionals and 12 other functionals, Theor. Chem. Acc. 120 (1–3) (2008) 215–241.
[24] C. Møller, M.S. Plesset, Note on an approximation treatment for many-electron systems, Phys. Rev. 46 (1934) 618–622.
[25] M.W. Schmidt, K.K. Baldridge, J.A. Boatz, S.T. Elbert, M.S. Gordon, J.H. Jensen, S. Koseki, N. Matsunaga, K.A. Nguyen, S. Su, T.L. Windus, M. Dupuis, J.A. Montgomery, General atomic and molecular electronic structure system, J. Comput. Chem. 14 (11) (1993) 1347–1363.
[26] M.S. Gordon, M.W. Schmidt, Advances in electronic structure theory: {GAMESS} a decade later, in: C.E. Dykstra, G. Frenking, K.S. Kim, G.E. Scuseria (Eds.), Theory and Applications of Computational Chemistry, Elsevier, Amsterdam, 2005, pp. 1167–1189 (Chapter 41).
[27] T.-T. Wu, X.-F. Wang, M.-X. Zhai, H. Liu, L. Zhou, Y.-J. Jiang, Negative differential spin conductance in doped zigzag graphene nanoribbons, Appl. Phys. Lett. 100 (5) (2012) 052112.
[28] P. Srivastava, N. Jaiswal, G.K. Tripathi, Chlorine sensing properties of zigzag boron nitride nanoribbons, Solid State Commun. 185 (2014) 41–46.
[29] J.C. Meyer, A.K. Geim, M.I. Katsnelson, K.S. Novoselov, T.J. Booth, S. Roth, The structure of suspended graphene sheets, Nature 446 (2007) 60–63.
[30] A.K. Geim, K.S. Novoselov, The rise of graphene, Nat. Mater. 6 (2007) 183–191.